

# Modal Testing and Model Validation Issues of SWiFT Turbine Tests

Timothy Marinone and David Cloutier  
ATA Engineering, San Diego, CA, 92130

Bruce LeBlanc  
Sandia National Laboratories,<sup>1</sup> Albuquerque, NM, 87185

## ABSTRACT

Sandia National Laboratories is developing the Scaled Wind Farm Technology center to enable rapid, cost-efficient testing and development of transformative wind energy technology. ATA Engineering, Inc., was contracted as part of this effort to dynamically characterize a number of components and assemblies to be used at the Scaled Wind Farm Technology center.

This paper documents several of the tests that were performed and describes the approaches, results, and challenges encountered during testing. The test articles that were dynamically characterized are the Vestas V27 wind turbine blades, Vestas V27 towers in a free-free boundary condition, and Vestas V27 towers in a bolted condition.

## INTRODUCTION

Sandia National Laboratories (SNL) is developing the Scaled Wind Farm Technology (SWiFT) center to enable rapid, cost-efficient testing and development of transformative wind energy technology. The site is intended to study complex turbine wake interactions and focus on damage mitigation, improved power performance, and recommended future site layouts. Since this site is designed to be open source and to provide data to all interested parties, the models must be accurate enough to be used for the desired analyses while preserving the proprietary information from Vestas. As such, ATA Engineering, Inc., (ATA) was contracted as part of this effort to dynamically characterize a number of components and assemblies to be used at SWiFT.

The SWiFT site consists of three modified 225 kW Vestas V27 (V27) turbines that were reworked by SNL. ATA characterized all major components of the turbine in order to provide test-verified data for use in updating SNL's models. This paper focuses on the testing of three components: the V27 wind turbine blades in a free-free boundary condition, the V27 towers in a free-free boundary condition, and the V27 towers in a bolted boundary condition. Additional papers [1, 2, 3] focus on the testing of the remaining components (hub and nacelle) testing the fully assembled turbine, and summarize the overall test program. The objective of this paper is to present the results of the tests described above.

## TEST ARTICLE—WIND TURBINE BLADES

The Vestas V27 (V27) wind turbine blades are thirteen meters long with a half-meter-diameter root section. These blades had been retired from the field after many years in service, and significant rework and repair were performed to make them functional again. Multiple sensors were installed into the blades to provide data at multiple points along the blades. Figure 1 shows an overall view of the blade, with a zoomed-in rework section and the test-display model used for mode visualization.

---

<sup>1</sup> Sandia is a multiprogram laboratory operated by Sandia Corporation, a Lockheed Martin Company, for the U.S. Department of Energy under Contract DE-AC04-94AL85000.

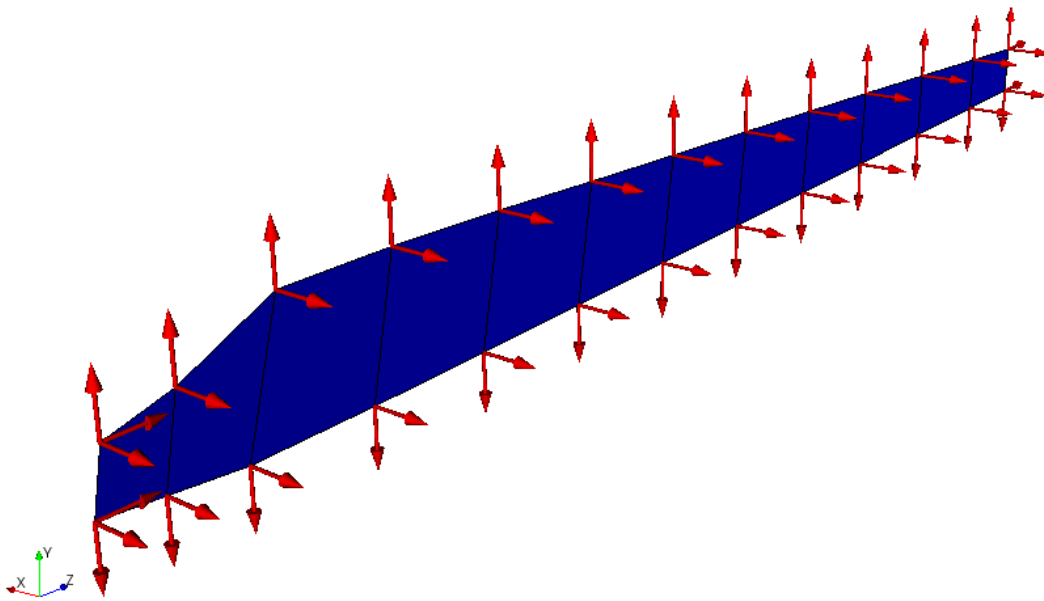
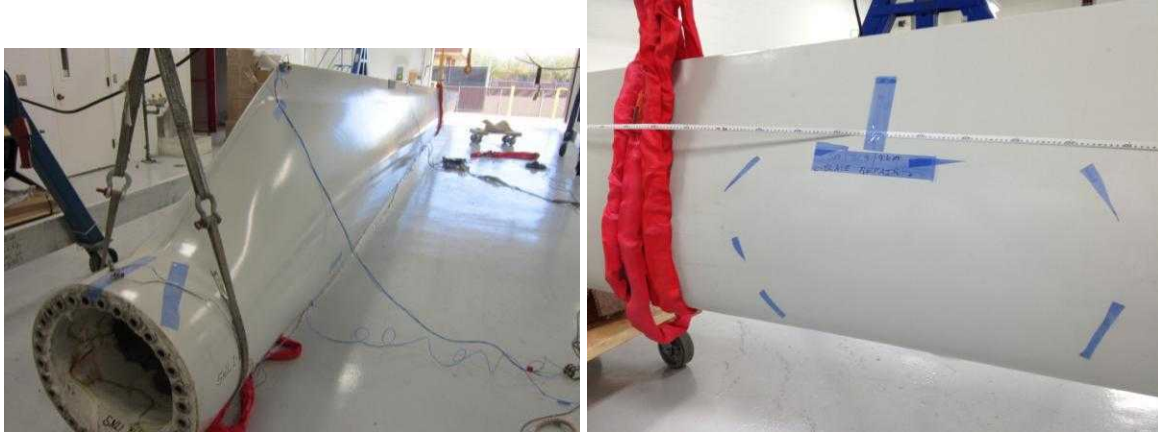


Figure 1. Overall view of the blade (upper left), zoomed-in section showing rework (upper right), and test-display model showing sensor locations (bottom).

The mass and CG of the blades were obtained by using two calibrated load cells at known distances along the blade to rigidly suspend the blade and record the load measured at each location. The mass moment of inertia was obtained by suspending the blade from two equal-length cords equidistant from the CG and measuring the period of oscillation about the desired axis. The following equation can then be used to solve for the mass moment of inertia term where the variables needed are the weight ( $W$ ), length of the rigid strap ( $L$ ), distance from the CG to the strap ( $x$ ), and period of oscillation ( $T$ ).

$$I = \frac{Wx^2T^2}{L} \frac{1}{4\pi^2}.$$

Equation 1

## TEST RESULTS—WIND TURBINE BLADES

This section documents the wind turbine blade test results. Figure 2 shows the FRF for the tip drive point in the flap direction and indicates a high-quality measurement due to the near-unity coherence and distinct resonance peaks.

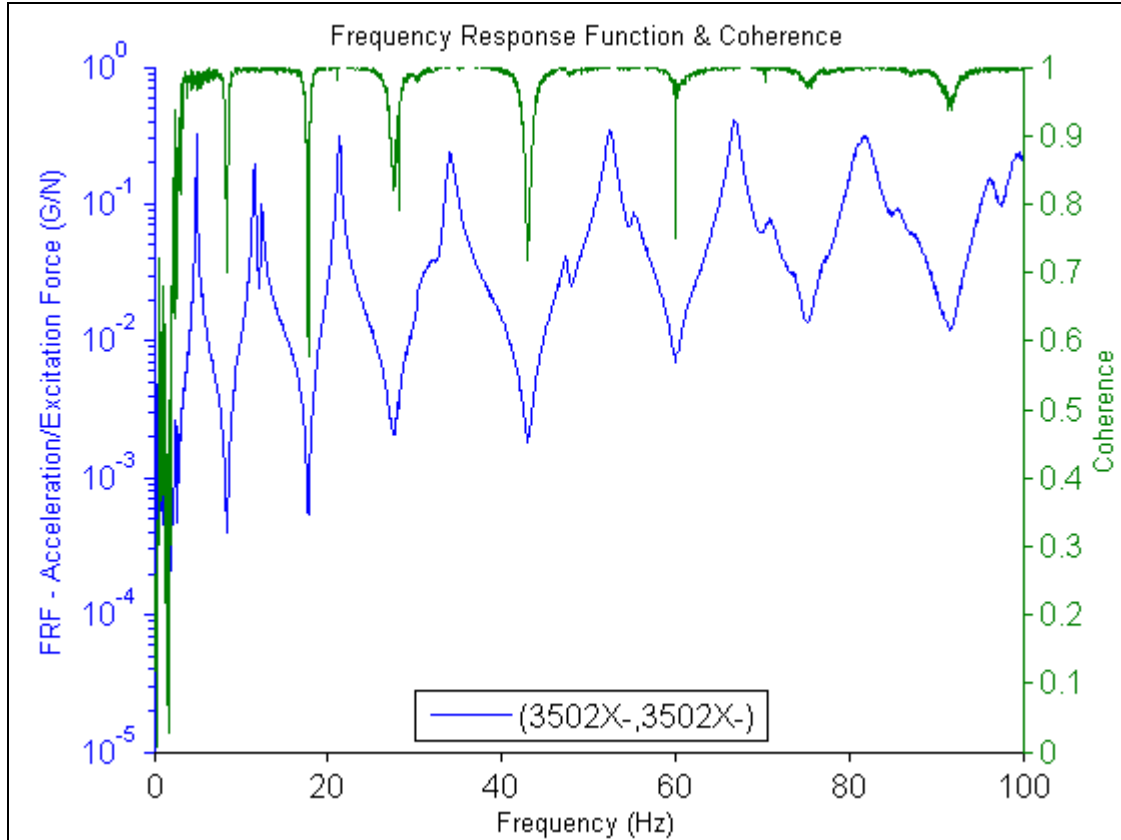


Figure 2. FRF and coherence for impact hammer drive point node (3502X-).

Table 1 lists the weight, CG, and moment of inertia about the y-axis for all six blades. Due to the multiple rotor sets, the manufacturing variability in older turbine blades, and the significant rework performed on several of the blades, the variation in weight and CG between blades is noticeable (8%). Because the moment of inertia is affected by both the CG and weight, its variation between blades is more significant (19%).

Table 1. V27 wind turbine blades' mass and inertia properties.

	SNL1_BL1	SNL1_BL2	SNL1_BL3	SNL2_BL1	SNL2_BL2	SNL2_BL3	Average	Max Difference (%)
<b>Weight (N)</b>	6343	6357	6303	6552	6423	6787	<b>6460.8</b>	<b>7.7</b>
<b>CG - X Axis (m)</b>	-	-	-	-	-	-	-	-
<b>CG - Y Axis (m)</b>	-	-	-	-	-	-	-	-
<b>CG - Z Axis (m)</b>	4.18	4.15	4.19	4.29	4.16	4.20	<b>4.20</b>	<b>3.4</b>
<b>Ixx (kg*m<sup>2</sup>)</b>	-	-	-	-	-	-	-	-
<b>Iyy (kg*m<sup>2</sup>)</b>	5002.8	5466.0	5097.4	4967.0	5887.3	5796.4	<b>5369.5</b>	<b>18.5</b>
<b>Izz (kg*m<sup>2</sup>)</b>	-	-	-	-	-	-	-	-
* Coordinate System Origin Defined at Blade Root Center								

Table 2 lists the frequency for all six wind turbine blades. The flapwise and edgewise modes have minimal variation (5%) between all six blades, indicating that the blades have a high degree of similarity. The torsion modes have a much higher variation (13%), which indicates that these modes are more sensitive to the rework. Table 3 shows an orthogonality comparison performed between the two blades that contained a full set of instrumentation; note that there are high-orthogonality terms between the two sets of modes.

Table 2. V27 wind turbine blades' modes sorted by test frequency.

Mode #	Description	Blade Frequency (Hz)						Average (Hz)	Max Difference (%)
		SNL1 - BL1	SNL1 - BL2	SNL1 - BL3	SNL2 - BL1	SNL2 - BL2	SNL2 - BL3		
1	1st Flapwise	4.79	4.80	4.94	4.90	4.82	4.88	4.86	3.16
2	2nd Flapwise	11.30	11.40	11.89	11.64	11.41	11.55	11.53	5.27
3	1st Edgewise	12.35	12.37	12.67	12.66	12.29	12.35	12.45	3.08
4	3rd Flapwise	21.49	21.40	21.97	21.54	21.69	21.29	21.56	3.19
5	2nd Edgewise	30.10	29.96	30.86	31.05	30.59	30.26	30.47	3.64
6	1st Torsion	34.70	30.58	31.08	33.11	32.40	32.43	32.38	13.47
7	4th Flapwise	33.60	34.24	34.90	34.64	34.64	34.04	34.34	3.88
8	2nd Torsion	50.46	47.75	48.66	50.02	51.69	52.53	50.19	10.01
9	3rd Edgewise	55.36	55.50	57.74	56.89	56.10	55.19	56.13	4.62

Table 3. V27 final test modes (SNL2\_BL1 and SNL2\_BL3 at full instrumentation set): self-orthogonality.

		Test Self Orthogonality Table																			
		Test Shapes		SNL2_BL1								SNL2_BL3									
		Ott	1	2	3	4	5	6	7	8	9	10	11	12	13	14	15	16	17	18	
Test Shapes	1	4.9	1.00																		
	2	11.6		1.00																	
	3	12.7			1.00																
	4	21.5				1.00															
	5	31.1					1.00														
	6	33.1						1.00	0.56												
	7	34.6							0.56	1.00											
	8	50.0									1.00										
	9	56.9										1.00									
SNL2_BL1	10	4.9	0.99									1.00									
	11	11.5		0.99									1.00								
	12	12.3			0.99										1.00						
	13	21.3				0.97										1.00					
	14	30.3					0.87										1.00				
	15	32.4						0.98										1.00	0.61		
	16	34.0							0.69	0.98										1.00	
	17	52.5									0.98										1.00
	18	55.2										0.52	0.95								0.51
SNL2_BL3	18	55.2																			0.51

The SNL V27 wind turbine blade model was updated to better reflect the actual blades based on the test results. The thickness of layup materials as well as the density of resin was used to match the mass, CG location, static deflection, and modal parameters. The comparison of the model results to test data is listed in Table 4.

Table 4. V27 wind turbine blade model correlation results

	Mass (kg)	CG (m)	1 <sup>st</sup> Flapwise (Hz)	2 <sup>nd</sup> Flapwise (Hz)	1 <sup>st</sup> Edgewise (Hz)
<b>Model</b>	641.9	4.31	4.82	10.09	12.56
<b>Average Experimental</b>	659.2	4.195	4.86	11.53	12.45
<b>Percent Difference</b>	-2.63%	2.74%	-0.8%	-12.5%	0.9%

**TEST ARTICLE—WIND TURBINE TOWERS**

The Vestas V27 (V27) towers are thirty-one meters long, made of a steel alloy, and weigh approximately 13 tons (26,000 lbs). The overall view of the tower and the test-display model used for mode visualization are shown in Figure 3 in the simulated free-free configuration. The towers were supported on frames located approximately at the nodes of the first bending mode, and during testing, airbags were inserted into the frames and used to lift the tower at four points to simulate a free-free boundary condition. Figure 4 shows the overall view of the towers bolted to the foundation and the corresponding test-display model.

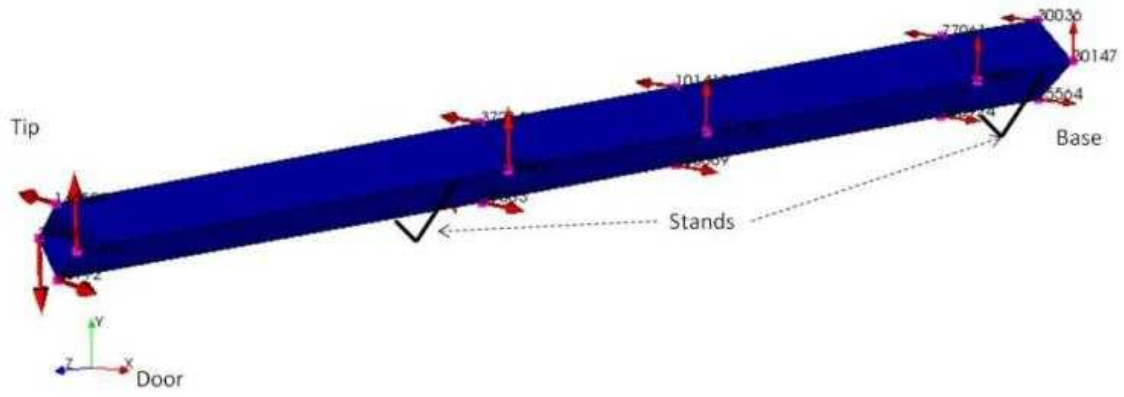


Figure 3. Overall view of the tower (left), support stand with airbags (right), and test-display model (bottom) in the free-free configuration.

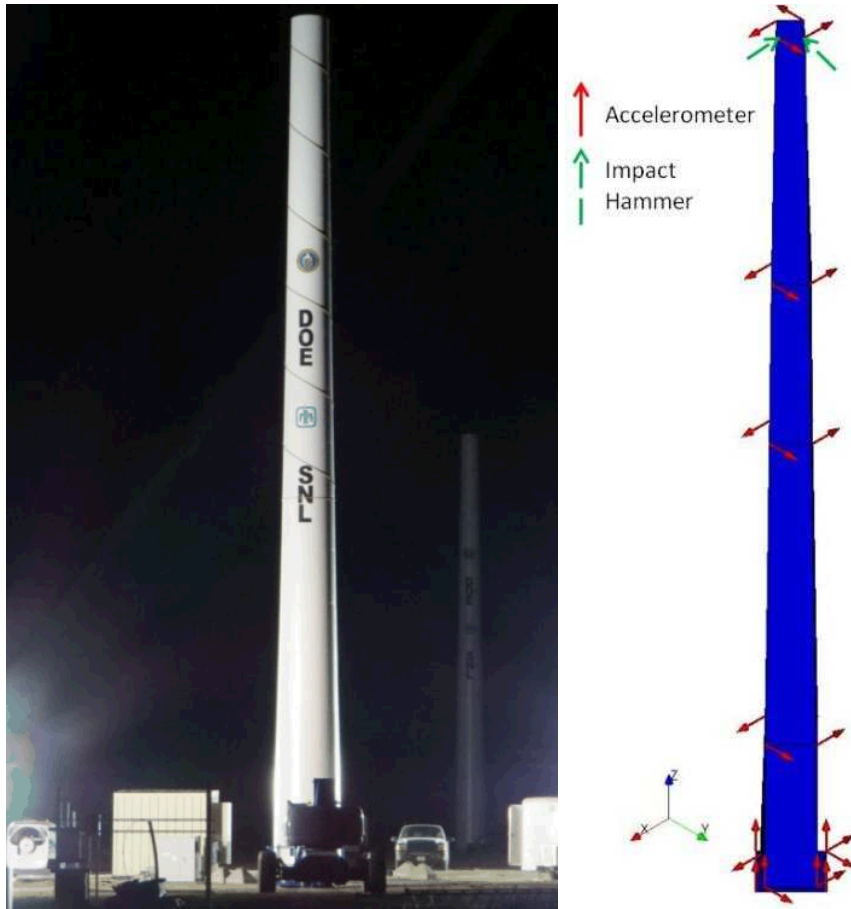


Figure 4. Overall view of the tower (left) and test-display model (right) in the bolted configuration.

## TEST RESULTS—WIND TURBINE TOWERS

This section documents the wind turbine tower test results. Figure 5 shows the FRF for the tip drive point and indicates a high-quality measurement due to the near-unity coherence and distinct resonance peaks.

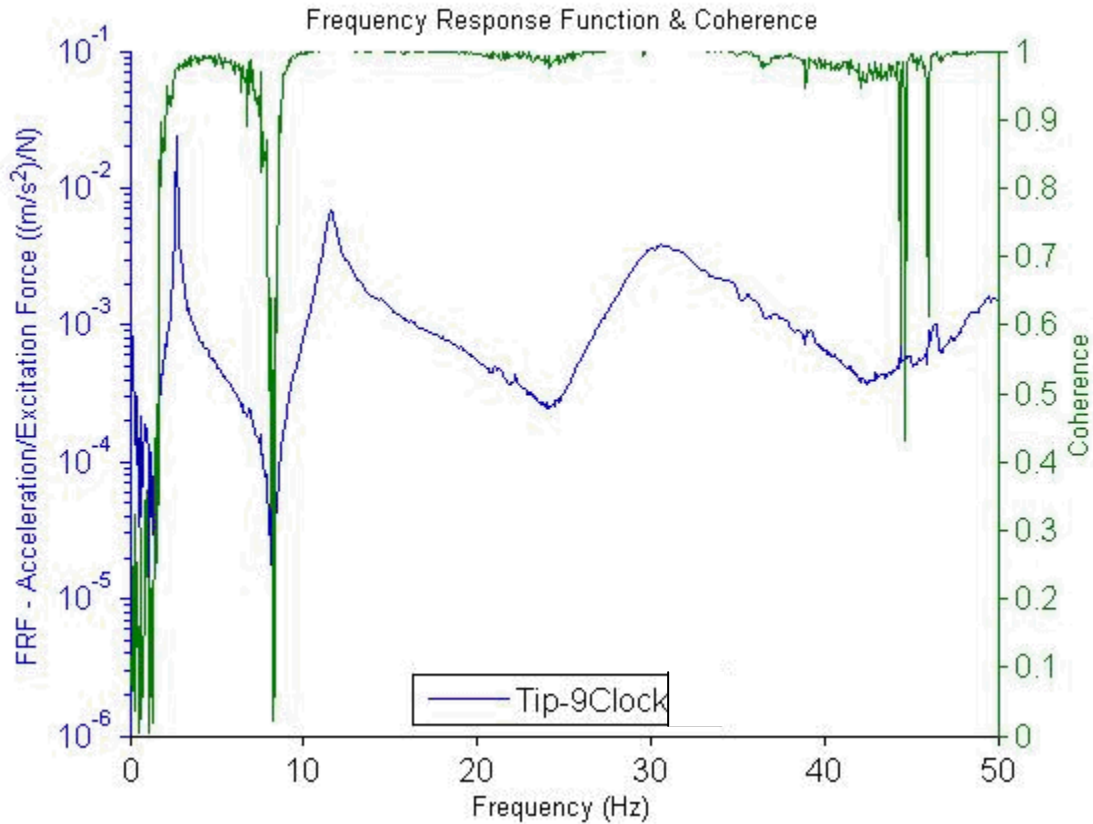


Figure 5. FRF and coherence for impact hammer drive point 3502X-, run 22.

Table 5 lists the frequency differences between the two towers in the free-free configuration, and Table 6 lists the frequency differences between the two towers in the bolted configuration. Although the frequencies and damping of the mode shapes compare well for the tower in the free-free boundary condition, the towers were oriented differently on the support stands. As a result, the orthogonal axes of bending were different, causing the corresponding mode shape vectors to be oriented at different angles. This led to poor MAC values, which are therefore not shown. When the towers were tested in a bolted configuration, however, they were oriented the same, and the mode shapes were compared and found to be very similar (MAC > 90) for the first bending mode.

Table 5. V27 wind turbine tower modes sorted by test frequency: free-free boundary condition.

	Tower 1		Tower 2	
	Frequency (Hz)	Damping (% Crit)	Frequency (Hz)	Damping (% Crit)
First Bending Mode	10.66	1.47	10.61	1.10
	10.88	2.47	10.69	1.92
Second Bending Mode	28.34	3.06	28.29	0.85
	29.10	2.24	28.80	1.09
Rigid Body Mode	2.12	6.86	2.08	5.48

Table 6. V27 wind turbine tower modes sorted by test frequency: bolted boundary condition.

	Axis of Motion	Tower 1		Tower 2		MAC
		Frequency (Hz)	Damping (% Crit)	Frequency (Hz)	Damping (% Crit)	
First Bending Mode	Fore-Aft (X)	2.70	0.56	2.61	0.82	0.95
	Side-Side (Y)	2.73	0.98	2.67	0.50	0.90
Second Bending Mode	Fore-Aft (X)	11.58	2.24	11.32	2.49	0.81
	Side-Side (Y)	11.71	1.76	11.58	1.57	0.84

In addition to verifying that the towers were similar, effort was focused on characterizing the foundation stiffness. Most modelers assume that the foundation is completely fixed, which introduces error. Thus, to determine the foundation stiffness, seismic accelerometers (393B04) were mounted on the concrete foundation in the vertical direction. Accelerometers were also mounted on the base of the tower to determine if there was relative motion between the tower and the foundation. A comparison of the FRFs from the two accelerometers is shown in Figure 6

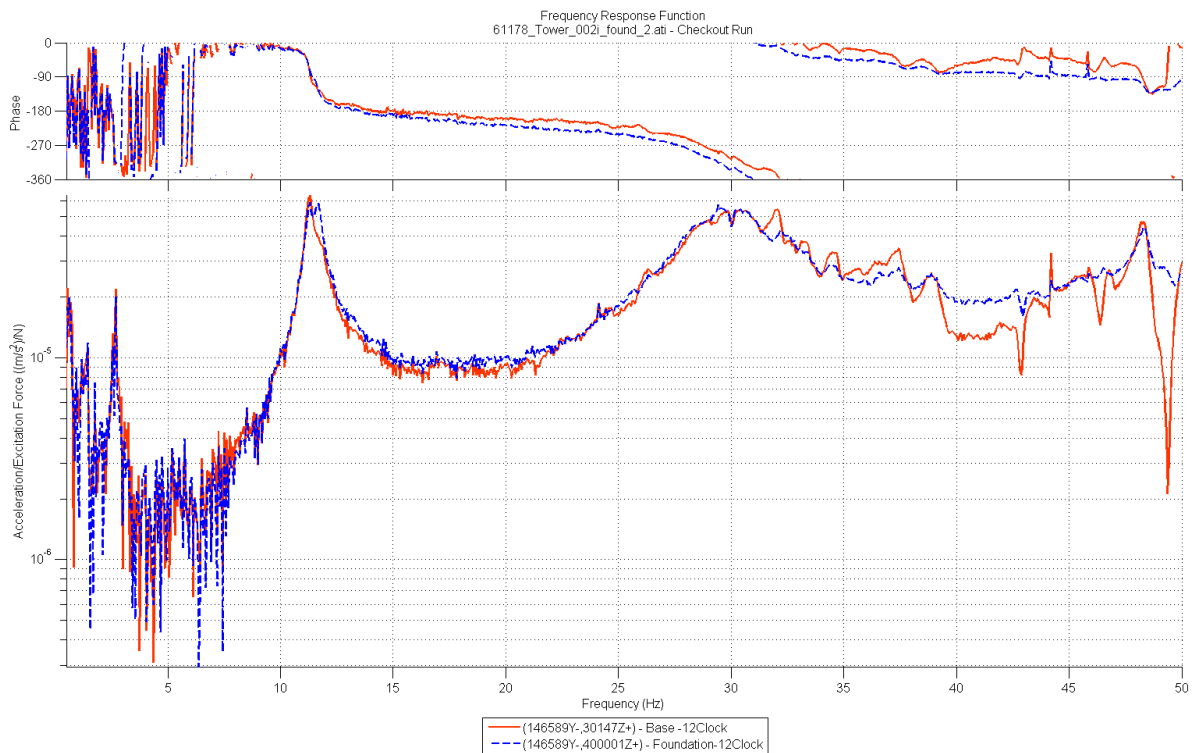


Figure 6. Comparison of FRFs between vertical accelerometers on tower foundation and tower base.

The FRF comparison shows minimal difference between the two accelerometers, which indicates that there is no relative motion between the tower and foundation. There is a clear natural frequency near 12 Hz, however, indicating that the foundation cannot be assumed to be completely fixed. Based on this information and the modal results from above, the tower boundary condition was changed from fixed to translational and rotary springs. A translational spring of 2 GN/m representing the horizontal stiffness of the foundation and a rotational spring of 13 GN-m/rad to represent the rocking stiffness were applied to a representative two-dimensional beam model of the tower. The results are shown in Table 7.

Table 7. V27 wind turbine tower model correlation results

Mode	Experimental (Hz)	Model (Hz)	% Difference	MAC
Mode 1	2.68	2.67	-0.3	.99
Mode 2	11.55	11.92	3.2	.98

## SUMMARY

This paper presented the results obtained from testing multiple components of the SWiFT V27 wind turbine.

The first test was on the six wind turbine blades, and the mass inertia and dynamic characteristics were obtained. The blades showed noticeable variation in mass and CG due to the rework done on the blades; the effects of this rework were also clearly seen in the torsional modes.

The second test was on the two wind turbine towers in both the free-free and bolted boundary conditions. Measurements taken on the foundation showed that the foundation was not fixed, and the boundary condition was updated to reflect the motion of the foundation.

The results obtained from these tests allow Sandia's wind turbine models to be more accurate for use in future analyses.

## REFERENCES

1. T. Marinone, K. Napolitano, D. Cloutier, and B. LeBlanc, "Comparison of Multiple Mass Property Estimation Techniques on SWiFT Vestas 27 Wind Turbine Nacelles and Hubs," *Proceedings of 32<sup>nd</sup> IMAC*, Orlando, Florida, 2014.
2. D. Cloutier, T. Marinone, B. LeBlanc, P. Anderson, and T. Carne, "Artificial and Natural Excitation Testing of SWiFT Vestas 27 Wind Turbines," *Proceedings of 32<sup>nd</sup> IMAC*, Orlando, Florida, 2014.
3. B. LeBlanc, D. Cloutier, and T. Marinone, "Overview of the Dynamic Characterization at the SWiFT Wind Facility," *Proceedings of 32<sup>nd</sup> IMAC*, Orlando, Florida, 2014.